Exogenous H₂S promotes ubiquitin-mediated degradation of SREBP1 to alleviate diabetic cardiomyopathy via SYVN1 S-sulfhydration

Shiwu Zhang[1] (iD), Mengyi Wang[1], Hongxia Li[1], Qianzhu Li[1], Ning Liu[1], Shiyun Dong[1], Yajun Zhao[1], Kemiao Pang[1], Jiayi Huang[1], Cheng Ren[2], Yan Wang[2], Zhen Tian[1], Fanghao Lu[1]* & Weihua Zhang[1]*

[1]*Department of Pathophysiology, Harbin Medical University, Harbin, China;* [2]*Department of Urologic Surgery, First Affiliated Hospital of Harbin Medical University, Harbin, China*

Abstract

Background   Diabetic cardiomyopathy, a distinctive complication of diabetes mellitus, has been correlated with the presence of intracellular lipid deposits. However, the intricate molecular mechanisms governing the aberrant accumulation of lipid droplets within cardiomyocytes remain to be comprehensively elucidated.
Methods   Both obese diabetic (db/db) mice and HL-1 cells treated with 200 μmol/L palmitate and 200 μmol/L oleate were used to simulate type 2 diabetes conditions. Transmission electron microscopy is employed to assess the size and quantity of lipid droplets in the mouse hearts. Transcriptomics analysis was utilized to interrogate mRNA levels. Lipidomics and ubiquitinomics were employed to explore the lipid composition alterations and proteins participating in ubiquitin-mediated degradation in mice. Clinical data were collected from patients with diabetes-associated cardiomyopathy and healthy controls. Western blot analysis was conducted to assess the levels of proteins linked to lipid metabolism, and the biotin-switch assay was employed to quantify protein cysteine S-sulfhydration levels.
Results   The administration of H₂S donor, NaHS, effectively restored hydrogen sulfide levels in both the cardiac tissue and plasma of db/db mice (+7%, $P < 0.001$; +5%, $P < 0.001$). Both db/db mice (+210%, $P < 0.001$) and diabetic patients (+83%, $P = 0.22$, $n = 5$) exhibit elevated plasma triglyceride levels. Treatment with GYY4137 effectively lowers triglyceride levels in db/db mice (-43%, $P = 0.007$). The expression of cystathionine gamma-lyase and HMG-CoA reductase degradation protein 1 (SYVN1) was decreased in db/db mice compared with the wild-type mice (cystathionine gamma-lyase: -31%, $P = 0.0240$; SYVN1: -35%, $P = 0.01$), and NaHS-treated mice (SYVN1: -31%, $P = 0.03$). Conversely, the expression of sterol regulatory element-binding protein 1 (SREBP1) was elevated (+91%, $P = 0.007$; +51%, $P = 0.03$ compared with control and NaHS-treated mice, respectively), along with diacylglycerol *O*-acyltransferase 1 (DGAT1) (+95%, $P = 0.001$; +35%, $P = 0.02$) and 1-acylglycerol-3-phosphate *O*-acyltransferase 3 (AGPAT3) (+88%, $P = 0.01$; +22%, $P = 0.32$). Exogenous H₂S led to a reduction in lipid droplet formation (-48%, $P < 0.001$), restoration of SYVN1 expression, modification of SYVN1's S-sulfhydration status and enhancement of SREBP1 ubiquitination. Overexpression of SYVN1 mutated at Cys115 decreased SREBP1 ubiquitination and increased the number of lipid droplets.
Conclusions   Exogenous H₂S enhances ubiquitin-proteasome degradation of SREBP1 and reduces its nuclear translocation by modulating SYVN1's cysteine S-sulfhydration. This pathway limits lipid droplet buildup in cardiac myocytes, ameliorating diabetic cardiomyopathy.

Keywords   Diabetic cardiomyopathy; Hydrogen sulfide; Lipid droplets; Sterol regulatory element binding protein 1; Synoviolin

Introduction

The global prevalence of type 2 diabetes is on the rise, and it currently ranks as the seventh leading cause of death, with cardiovascular complications being the primary contributor.[1] Over five decades ago, the Framingham Heart Study underscored diabetes as a significant contributor to heart failure.[2] Diabetic cardiomyopathy has been defined as impairments of cardiac structure and function independent of coronary artery disease, hypertension and atherosclerosis. Accumulating evidence has supported that intrinsic abnormalities in cardiomyocyte energy use and lipid metabolism result in diabetic cardiomyopathy.[3,4] Free fatty acids (FFAs) uptake and oxidative levels are significantly up-regulated in cardiomyocytes of type 2 patients, while glucose uptake is decreased.[5] Excessive FFAs can store as lipid droplets (LDs) in the heart, potentially causing dysfunction and heart failure.[6] Human studies have implicated myocardial lipid accumulation in diabetic cardiac dysfunction.[7] Nevertheless, the underlying mechanisms remain to be fully elucidated.

Sterol regulatory element-binding proteins (SREBPs) are a family of transcription factors that regulate lipid homeostasis. SREBPs have three isoforms in most cells, including SREBP-1a, SREBP-1c and SREBP-2, which have their own physiological and pathological roles in lipid synthesis.[8] In vivo studies using transgenic and knockout mice have shown that SREBP-1c is involved in FFA synthesis and insulin-induced glucose metabolism (especially lipogenesis), whereas SREBP-2 is relatively specific for cholesterol synthesis. The SREBP-1a isoform appears to be involved in both pathways.[9] SREBPs undergo transportation from the endoplasmic reticulum (ER) to the Golgi apparatus and proteolytic processing.[10] SREBPs generate soluble N-terminal cleavage transcription factors of the basic helix–loop–helix leucine zipper family, which enable SREBP to enter the nucleus as a homodimer, bind to SRE sequences and stimulate transcription of target genes.[8] Recent studies have shown that valosin-containing protein recognizes ubiquitinated SREBP1 and facilitates its proteolytic processing. SREBP1 may be involved in the regulation of the ubiquitin-proteasome degradation system, thereby regulating lipid synthesis.[11]

Numerous studies revealed the significant protective role of hydrogen sulfide at low concentrations in vivo.[12] The enzymes that catalyse endogenous H_2S mainly include cystathionine-β-synthase (CBS), cystathionine-γ-lyase (CSE) and 3-mercaptopyruvate thiotransferase (3-MST, also known as MPST).[13] H_2S plays important roles in many physiological and pathological processes, including oxidative stress,[14] autophagy[15] and ER stress.[16] Endogenous H_2S catalysed by CSE is significantly inhibited in cardiomyocytes of rats with diabetic cardiomyopathy.[17]

Cysteine S-sulfhydration is a post-translational modification introduced into protein molecules through oxidative reactions, thereby introducing thiol (–SH) groups and extensively regulating various biological processes within cells.[18] Serving as active sites within protein molecules, cysteine residues play critical roles not only in protein folding and stability but also in the regulation of numerous cellular signalling pathways. In recent years, it has become evident that protein cysteine S-sulfhydration modification plays significant roles in cellular stress responses, metabolic adaptations and disease development.[19]

The E3 ubiquitin ligase HMG-CoA reductase degradation protein 1, also known as Synoviolin-1 (SYVN1/Hrd1), is a critical component of the cellular protein quality control machinery. It plays a pivotal role in the ER-associated degradation pathway, which is responsible for identifying and disposing of misfolded or unassembled proteins within the ER.[20] SYVN1 operates by tagging these aberrant proteins with ubiquitin moieties, marking them for subsequent proteasomal degradation. Our prior study revealed that exogenous H_2S reduced lipid droplet accumulation in diabetic cardiomyopathy. Yet the mechanisms were unclear.[21] Our current research demonstrates that exogenous H_2S curtails lipid droplet buildup by enhancing the ubiquitin-mediated degradation of SREBP1 through up-regulating S-sulfhydration of SYVN1.

Methods

Animal models

Female mice with type 2 diabetes (db/db) aged 4–6 weeks and control mice (C57BL/6) were kept in a controlled environment (23–25°C, 12–12 h light–dark cycle). Diabetes was confirmed when blood glucose levels stayed >16.7 mmol/L for 3 days. Animals in the experimental cohort received intraperitoneal injections of NaHS at a dose of 4.8 mg/kg every 2 days. The NaHS injections were administered over a span of 16 weeks. Additionally, GYY4137 was administered through intraperitoneal injections for a duration of 4 weeks (133 μM/kg/day). All animals were sourced from Animal Model Experiment Center of Nanjing University, Nanjing, China, and experiments were conducted according to Harbin Medical University's Ethics Committee guidelines.

Cell culture

HL-1 cells were cultured in high-glucose DMEM with 10% fetal bovine serum. Passaging occurred at 80–90% confluence, and drug treatments were given at 50–60% confluence in the medium over 48 h. The cell treatments included the following: oleate (200 μmol/L), palmitate (200 μmol/L), NaHS (100 μmol/L), GYY4137 (100 μmol/L), PPG (10 μmol/L), 4-phenylbutyric acid (4-PBA, 5 mmol/L) and thapsigargin (Tg, 100 nmol/L). Palmitate solubility was improved with a

10% BSA solution, uniformly applied to both control and treatment groups at equivalent volumes and concentrations.

Measurement of H₂S levels

Hydrogen sulfide content in cells was assessed using the 7-azido-4-methylcoumarin probe (C7Az, Sigma) under 720 nm laser excitation, observed via a fluorescence microscope (Olympus, XSZD2). Quantification of hydrogen sulfide (H₂S) in cardiac tissue and serum employed the dedicated H₂S content Kit (Solarbio).

Western blot analysis

All protein samples were quantified by using the BCA reagent (Beyotime). Anti-CSE, anti-DGAT1, anti-SREBP1, anti-AGPAT3, anti-CHOP, anti-eIF2α, anti-PERK, anti-BIP, anti-β-Tubulin, anti-SYVN1 and anti-Ubiquitin were from Proteintech. Anti-P-eIF2α (Ser51) and anti-P-PERK (Thr980) were from Cell Signalling Technology. Specific bands were recorded via a chemiluminescence detection system (Thermo). The band intensity was conducted by ImageJ tool.

Immunofluorescence

Cells were plated on coverslips at a density of approximately 8000/cm², paraformaldehyde fixed cells for 30 min, permeabilized for 1 h at room temperature, incubated with primary antibodies overnight at 4°C, incubated with secondary antibodies for 1 h (protected from light) and recorded under a fluorescence microscope (Olympus, XSZD2).

BODIPY 493/503 staining and Oil Red O staining

Cells were incubated with 4% paraformaldehyde for 20–30 min and rinsed slowly with PBS three times. BODIPY 493/503 dye mixed with serum-free medium to a final concentration of 1 μg/mL and incubated the cells at 37°C in the dark for 30 min. After being rinsed carefully three times with PBS, the stained lipid droplets were recorded under a fluorescence microscope (Olympus, XSZD2).

Cells were fixed with 4% paraformaldehyde, washed with PBS and stained with Oil Red O working solution at room temperature for 15–30 min. After haematoxylin staining, cells were observed under fluorescence microscope.

Immunohistochemistry

The slides were deparaffinized in xylene twice for 5 minutes each, followed by transfer to 100% alcohol twice for 3 mi-
nutes each, then 95%, 70%, and 50% alcohols for 3 minutes each. Antigen retrieval was performed. Subsequently, the slides were treated with a blocking buffer (80 μL) and incubated for 1.5 hours. Afterward, diluted primary antibodies (anti-CSE, anti-CBS, and anti-MPST from Proteintech, 80 μL) were applied and incubated for 1 hour. Finally, diluted biotinylated secondary antibody (100 μL) was applied and incubated for 30 minutes.

Immunoprecipitation

Protein samples were incubated with anti-SREBP1, anti-ubiquitin or IgG antibodies and agarose (Santa) for 8 h at 4°C. The precipitates were collected after centrifugation at 10 000× g for 10 min and washed three times in IP buffer, resuspended in sample buffer and analysed by immunoblotting.

S-sulfhydration assay

The assay was carried out as described previously.[22] Briefly, tissue lysate for the sulfhydryl modification assay was prepared with a lysis buffer containing 250 mmol/L Hepes (pH 7.7), 100 μmol/L deferoxamine, 1 mmol/L EDTA, 100 μmol/L neocuproine, 0.5% (w/v) CHAPS, 0.1% (w/v) SDS, 10 μg/mL leupeptin, 5 μg/mL aprotinin and 1 mmol/L PMSF. After centrifugation, the supernatant was set to a protein concentration of 5 mg/200 μL. It was combined with blocking buffer (250 mmol/L Hepes, 1 mmol/L EDTA, 100 μmol/L neocuproine, 2.5% (w/v) SDS and 20 mmol/L MMTS), incubated at 50°C for 20 min, and proteins were precipitated using acetone at −20°C for 1 h. The protein precipitate was resuspended in HEN buffer (250 mmol/L Hepes, 1 mmol/L EDTA, 100 μmol/L neocuproine and 1 mg/mL SDS) and treated with Biotin-HPDP termination solution at 25°C for 1 h. Streptavidin agarose beads were added, incubated and washed, and proteins were eluted using an elution buffer (250 mmol/L Hepes, 100 mM NaCl, 1 mM EDTA and 100 mM mercaptoethanol) at 37°C for 20 min. Modified proteins were denatured, subjected to Western blotting analysis after preparation.

Generation of point mutation

Adenoviruses expressing GFP and SYVN1 were procured from Cyagen Biosciences Inc. (Guangzhou, China). We used a full-length mouse SYVN1 construct with a specific mutation: cysteine 115 was substituted with alanine. The purified adenovirus was administered through intravenous injection into mice via the tail vein. The adenoviruses were directly added to cells. Following a 6-hour transfection period, the medium was replaced with fresh DMEM medium. The cells were

treated 24 hours after transfection, and relevant proteins were subsequently detected.

Transcriptome sequencing

Each sample utilized 1 µg RNA for sample preparation. NEBNext UltraTM RNA Library Prep Kit for Illumina (NEB, USA) was employed for library creation, following manufacturer guidelines. Index codes were added to distinguish samples. Index-coded samples were clustered using TruSeq PE Cluster Kit v4-cBot-HS (Illumina) on a cBot Cluster Generation System. Subsequently, Illumina platform sequencing generated paired-end reads.

LC–MS/MS analysis for lipidomics and ubiquitylome

Using the UPLC–MS/MS platform, we employed a built-in database and MRM detection to qualitatively and quantitatively assess lipid metabolites in mouse heart samples. Data analysis involved multivariate statistical methods. Eighteen samples in three groups were studied, revealing 1313 detected metabolites.

For quantitative lysine ubiquitylome analysis, we used K-ε-GG standard peptides for affinity enrichment, followed by label-free quantitative proteomics. This was conducted on paired mouse myocardial tissues using three LC–MS/MS analyses in parallel.

Statistical analysis

In this experiment, Student's *t*-test was used to compare the means of the data between two samples, whereas the one-way ANOVA was used to compare the means of multiple samples. The data in this experiment were not <3 independent repeated experiments. All were expressed as mean ± standard error of the mean, and $P < 0.05$ was considered statistically significance. Statistical analysis was performed using Prism 9 (GraphPad, La Jolla, CA, USA). Software PyMol v.4.6.0 was used to generate the figures of all proteins.

Results

Exogenous H₂S alleviates cardiac function and hyperglycaemia in db/db mice

Diabetic mice (leptin receptor knockout mice, db/db) exhibited a marked increase in body weight compared with C57BL/6 mice and db/db mice treated with NaHS (a H₂S donor) (Figure 1A,B and Figure S1a). Furthermore, we con-

ducted an assessment of blood glucose levels, glucose tolerance and lipid profiles. Notably, db/db mice displayed notably elevated blood glucose (27.35 mmol/L), reflective of their diabetic state, whereas exogenous H₂S treatment alleviated the blood glucose level (Figure 1C,D and Figure S1b). In addition, db/db mice exhibited elevated triglyceride concentrations compared with wild-type mice (WT), db/db mice treated with NaHS, and those treated with GYY4137 (a slow-release H₂S agent) (Figure 1E and Figure S4c). Conversely, db/db mice displayed reduced high-density lipoprotein levels relative to db/db mice treated with NaHS (Figure 1F). Clinical data further demonstrate a significant elevation in triglyceride levels among patients with diabetic cardiomyopathy (Figure S4d). However, serum lipoproteins, creative and non-esterified fatty acids have no discernible alterations (Figure S1c–e). To investigate the effect of exogenous H₂S on cardiac functions, we measured haemodynamic parameters in anaesthetized mice by echocardiography. As shown in Figure S1f–h, left ventricular end-diastolic volume, left ventricular ejection fraction and left ventricular fractional shortening were clearly reduced in db/db mice compared with WT at 16 weeks, while the above indicators improved in the NaHS treatment group (db/db+NaHS). The left ventricular mass was clearly increased in db/db mice, and it was significantly restored after the administration of exogenous H₂S (Figure S1i).

Exogenous H₂S improves H₂S levels in cardiomyocytes

CSE is the primary enzyme for endogenous H₂S synthesis, particularly dominant in cardiac H₂S production.[23] Western blot analysis showed that CSE expression was greatly decreased in db/db mice at 16 weeks (Figure S2a, b). The content of H₂S in cardiac tissues of db/db group decreased significantly compared with WT and db/db mice treated with NaHS (Figure 2C). Notably, immunohistochemical evaluation further corroborated the significant diminishment of CSE expression within the hearts of db/db mice. However, the protein levels of CBS and MPST exhibited no significant alterations (Figure 2D and Figure S2d). Analysis of the transcriptomic data (GSE26887) of the cardiac tissues collected from healthy controls and diabetic patients showed that the mRNA levels of *CTH*, which encodes CSE, are significantly down-regulated (Figure 2E). Both db/db mice and diabetic patients exhibit a significant decrease in serum H₂S levels. Administration of NaHS effectively up-regulates hydrogen sulfide levels in db/db mice (Figure 2F and Figure S2c). In addition, HL-1 cells were treated with oleate and palmitate to mimic type 2 diabetic cardiomyopathy (Figure S3a, b). Subsequent analyses unveiled a reduction in CSE expression within the Pal+Ole group, when compared with the control group (Figure 2A, B). The H₂S probe, 7-azido-4-methylcoumarin (C-7Az), was
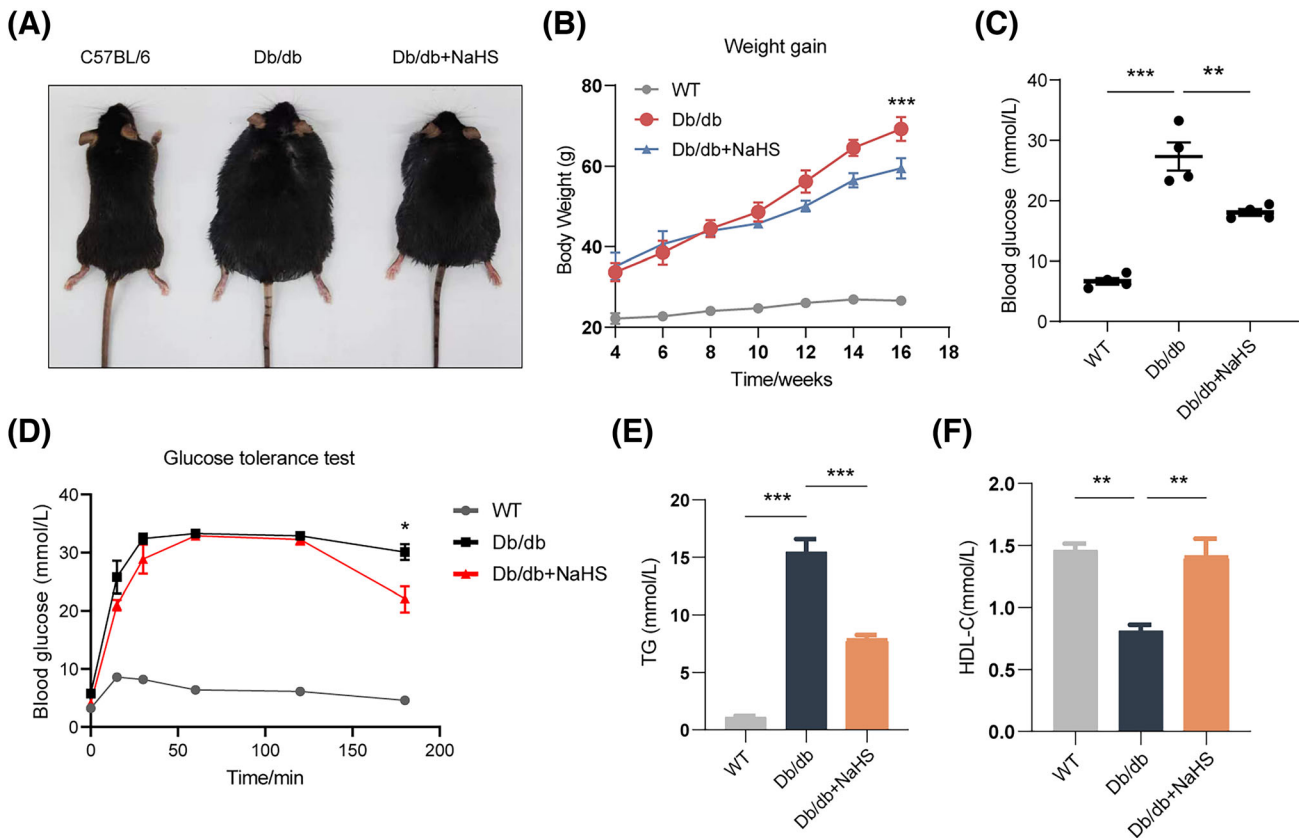
Figure 1 Exogenous H$_2$S ameliorated heart dysfunction in db/db mice. (A) Photograph of mice at 16 weeks. (B) Statistical results of body weight in 6- to 16-week-old db/db mice, control mice and db/db+NaHS mice (n = 5). (C, D) Statistical results of blood glucose and glucose tolerance at 16 weeks (n = 4). (E, F) Serum triglyceride and high-density lipoprotein content. Values are presented as mean ± SEM. *$P < 0.05$, **$P < 0.01$, ***$P < 0.001$.

used to dynamically detect the H$_2$S content of cardiomyocytes at 24, 48 and 72 h. Strikingly, the H$_2$S levels exhibited a discernible decline at each time point subsequent to Pal +Ole and PPG (a CSE inhibitor) treatment when contrasted with the control group. However, the H$_2$S levels were reinstated in the NaHS and GYY4137 groups (Figure S2e). Overall, these findings underscore reduced CSE expression and H$_2$S levels in cardiac tissues, diabetic animal models and cells. Diabetic patients also displayed lower H$_2$S levels, but exogenous H$_2$S administration showed a restorative effect.

Exogenous H$_2$S reduces the number of lipid droplets in cardiomyocytes and db/db mice

Subsequently, we embarked on investigating whether exogenous H$_2$S could alleviate lipid deposition in type 2 diabetic cardiomyopathy. The transmission electron microscopy results unveiled a progressive increase over time in both the number and dimensions of LDs in the cardiac tissues of db/ db mice, a pattern notably distinct from that observed in wild-type mice (as indicated by red arrows). Intriguingly, exogenous H$_2$S administration exerted a substantial reduction

in both LD number and size within the cardiac tissues of db/db mice (Figure 3A–C, Figure S4a, b). In both db/db mice and diabetic patients, there is a noteworthy elevation in plasma levels of triglycerides. However, treatment with GYY4137 significantly attenuates triglycerides levels in db/ db mice (Figure S4c, d). HE staining revealed the presence of a substantial number of vacuolar lipid droplets in the myocardial tissues, predominantly within the myofilaments and cardiomyocytes (Figure S3c). We further used BODIPY493/ 503 stain for LD detection in cardiomyocytes. The number of LDs increased in the Pal+Ole group at 24, 48 and 72 h compared with that in the control and NaHS-treated groups (Figure 3D, Figure S4e–i). High-resolution mass spectrometric lipid profiling of mouse hearts revealed three distinct clusters with respect to principal component analysis (Figure 3E). Among the differential metabolites, triglyceride (C43H80O6) and diglyceride (C37H74O4 and C39H78O4) exhibited a significant reduction in db/db mice treated with NaHS when contrasted with their db/db counterparts (Figure 3F). The above results collectively highlight a significant escalation in the number of lipid droplets within the cardiac tissues of type 2 diabetic mice, as well as in cardiomyocytes exposed to Pal +Ole. Conversely, exogenous H$_2$S reduced LDs effectively.
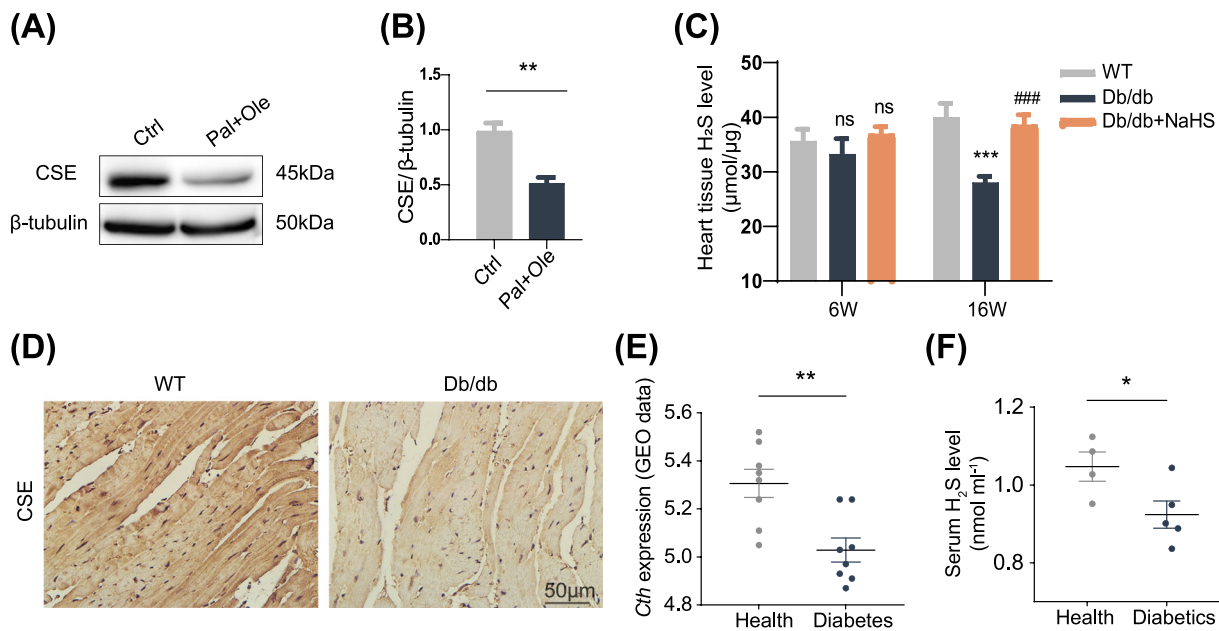
Figure 2 CSE expression and H$_2$S level in DCM. (A, B) Representative protein levels of CSE normalized to β-tubulin in HL1 cells (n = 3) by western blot. (C) Hydrogen sulfide level in myocardial tissue at 6 and 16 weeks. (D) Immunohistochemistry of CSE at 16 weeks. (E) GEO database transcriptomic analysis (GSE26887). (F) Plasma hydrogen sulfide levels in healthy controls and clinical patients with diabetes (n = 4–6). Values are presented as mean ± SEM. *P < 0.05, **P < 0.01, ***P < 0.001 versus control group, ###P < 0.001 versus Pal+Ole group.

Exogenous H$_2$S reduces the expression of SREBP1 and lipid-related proteins

An essential query we pursued was how H$_2$S reduced the number of LDs. To address this, we examined SREBP1, DGAT1 and AGPAT3 expression linked to lipid droplet synthesis in mouse cardiac tissues. db/db mice exhibited notably increased levels of these proteins compared with wild-type and db/db mice subjected to either GYY4137 or NaHS treatment (Figure 4A,B and Figure S5a, b). Similar findings were obtained in HL-1 cardiomyocytes, corroborating previous results. (Figure 4C). Previous studies have revealed that triglyceride synthesis in cardiomyocytes is mainly mediated by the transcription factor SREBP1, which is synthesized in the ER and processed in the Golgi. Mature cleaved nSREBP1 with nuclear localization signals enters the nucleus to exert its transcriptional regulatory function.[24] In order to ascertain the influence of exogenous H$_2$S on the nuclear translocation of nSREBP1 within cardiomyocytes, we meticulously assessed the expression levels of nSREBP1 specifically within the nucleus. Strikingly, discernible distinctions were observed, with the Pal+Ole group manifesting higher nSREBP1 expression relative to the control and NaHS groups (Figure 4D). Immunofluorescence showed that SREBP1 expression was significantly higher in the Pal+Ole group compared with the control or NaHS treated groups, and its nuclear translocation was also significantly increased (Figure 6B, Figure S7c). These findings collectively suggest that the administration of exogenous

H$_2$S has the capacity to effectively modulate the expression of lipid-associated proteins, thereby exerting a regulatory influence on this intricate process.

Exogenous H$_2$S decreases LD formation by alleviating endoplasmic reticulum stress

Through transcriptome analysis, we identified 8140 differentially expressed genes (fold change, FC > 2, P-adjust<0.05) between db/db and wild-type mice. The volcano plot shows the relative amounts of differentially expressed genes and the statistical significance of the differences in WT and db/db mice (Figure 5A). Gene enrichment analysis showed that differentially expressed genes were mainly involved in nuclear transport, enzyme activation and ubiquitin-proteasome degradation and were mainly located in the cytoplasm, nucleus and ER (Figure 5B). Previous studies have shown that the pathogenesis of diabetic cardiomyopathy is closely related to ER stress injury.[25,26] The occurrence of ER stress promotes abnormal accumulation of LDs in cells.[27] To ascertain whether exogenous H$_2$S inhibits ER stress and LDs generation in type 2 diabetes cardiomyopathy, we examined the changes in ER stress markers. Notably, our results, as demonstrated in Figure S6a, distinctly revealed elevated expression of proteins intricately associated with the ER stress pathway, including p-PERK, p-eIF2α, CHOP and BIP, within the cardiac tissues of db/db mice in contrast to their wild-type counterparts. Im-
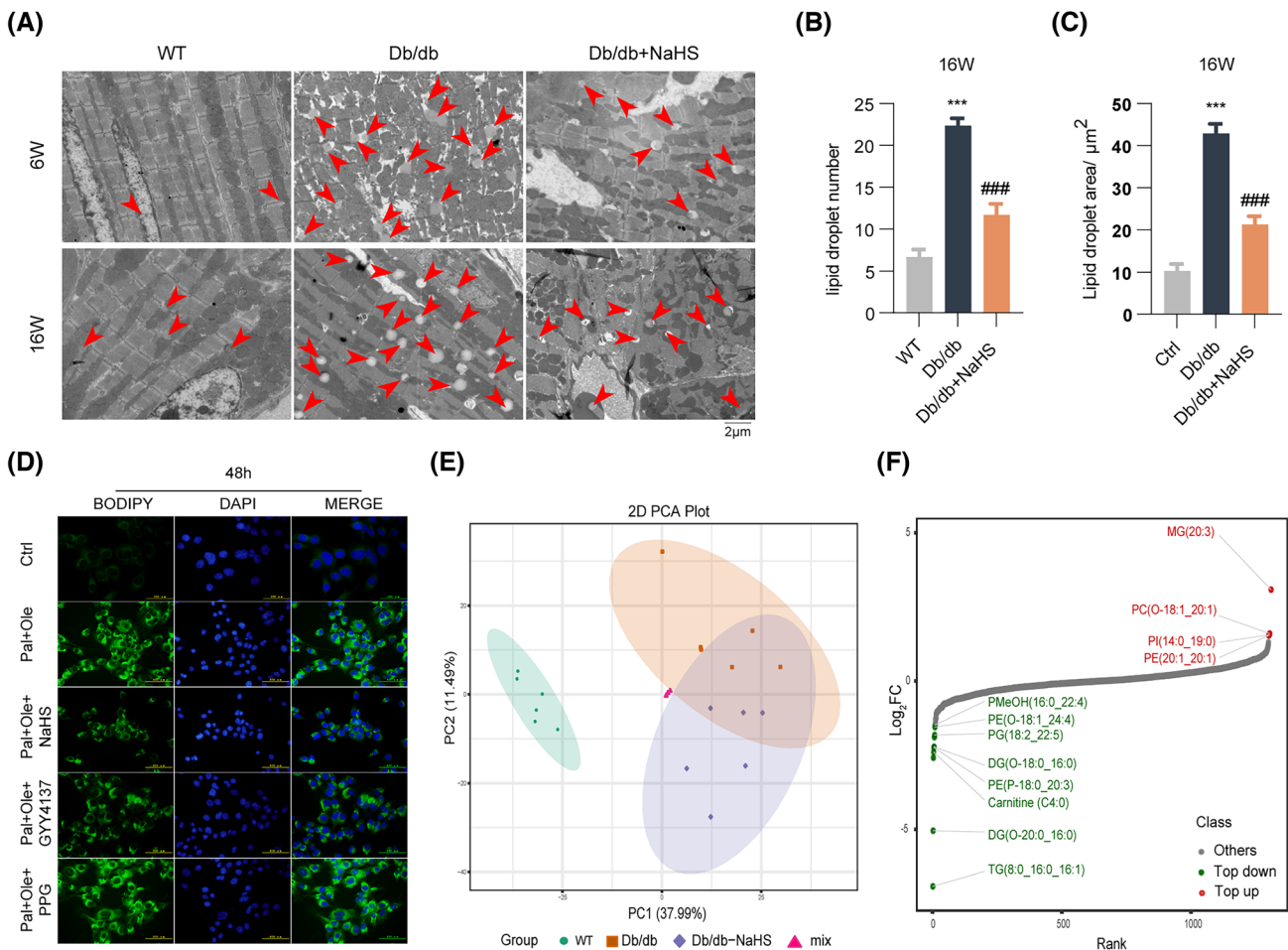
Figure 3 Exogenous H$_2$S alleviated lipid deposition in type 2 diabetic cardiomyopathy. (A–C) Transmission electron microscopy (TEM) of cardiac tissues of mice at 6 and 16 weeks. Lipid droplets are indicated by the red arrows (n = 3). (D) Lipid droplets in cardiomyocytes detected with the fluorescent probe BODIPY 493/503 (n = 4). (E) Principal component analysis of mice was conducted based on high-resolution mass spectrometric lipid profiling (n = 6). (F) Differential dynamic profiles of metabolite contents by fold change (FC) values. MG, monoglycerides; PC, phosphatidylcholine; PI, phosphoinositides; PE, phosphatidylethanolamine; PMeOH, phosphatidylmethanol; PG, phosphatidylglycerol. Values are presented as mean ± SEM. ***P < 0.001 versus control group, ###P < 0.001 versus db/db group.

portantly, exogenous H$_2$S effectively countered this elevated expression. To further determine the role of exogenous H$_2$S in high fatty acid-induced ER stress, we examined ER stress-related proteins in cardiomyocytes treated with Pal +Ole. The ER stress agonist Tg and the ER stress inhibitor 4-PBA were used as positive and negative controls, respectively. The expression of ER-related proteins was also increased in the Pal+Ole group compared with the control group, the NaHS group and the GYY4137 group (Figure 5C).

Next, we examined whether the accumulation of LDs was related to ER stress. We treated cardiomyocytes with the ER stress agonists Tg and tunicamycin (Tm). The BODIPY493/503 probe was used to detect the number of LDs in cardiomyocytes. We observed that the number of LDs accumulated gradually in a timedependent manner when Tg and Tm were used (Figure 5D, Figure S6b). Furthermore,

we observed a decrease in the number of LDs when 4-PBA and NaHS was used (Figure S6c, d).

Exogenous H$_2$S down-regulates SREBP1 expression by attenuating ER stress

To better understand the mechanisms by which ER stress can induce the accumulation of LDs, we conducted a rigorous analysis of the expression profiles of SREBP1 in the cytoplasm and the nuclear form of SREBP1 (nSREBP1) within the nucleus using Tg and 4-PBA. Figure 6A shows that SREBP1 expression was substantially increased in the Pal+Ole group and Tg group compared with the control group in the cytoplasm of cardiomyocytes. SREBP1 expression was clearly decreased in cardiomyocytes after treatment with NaHS and 4-PBA. Simi-
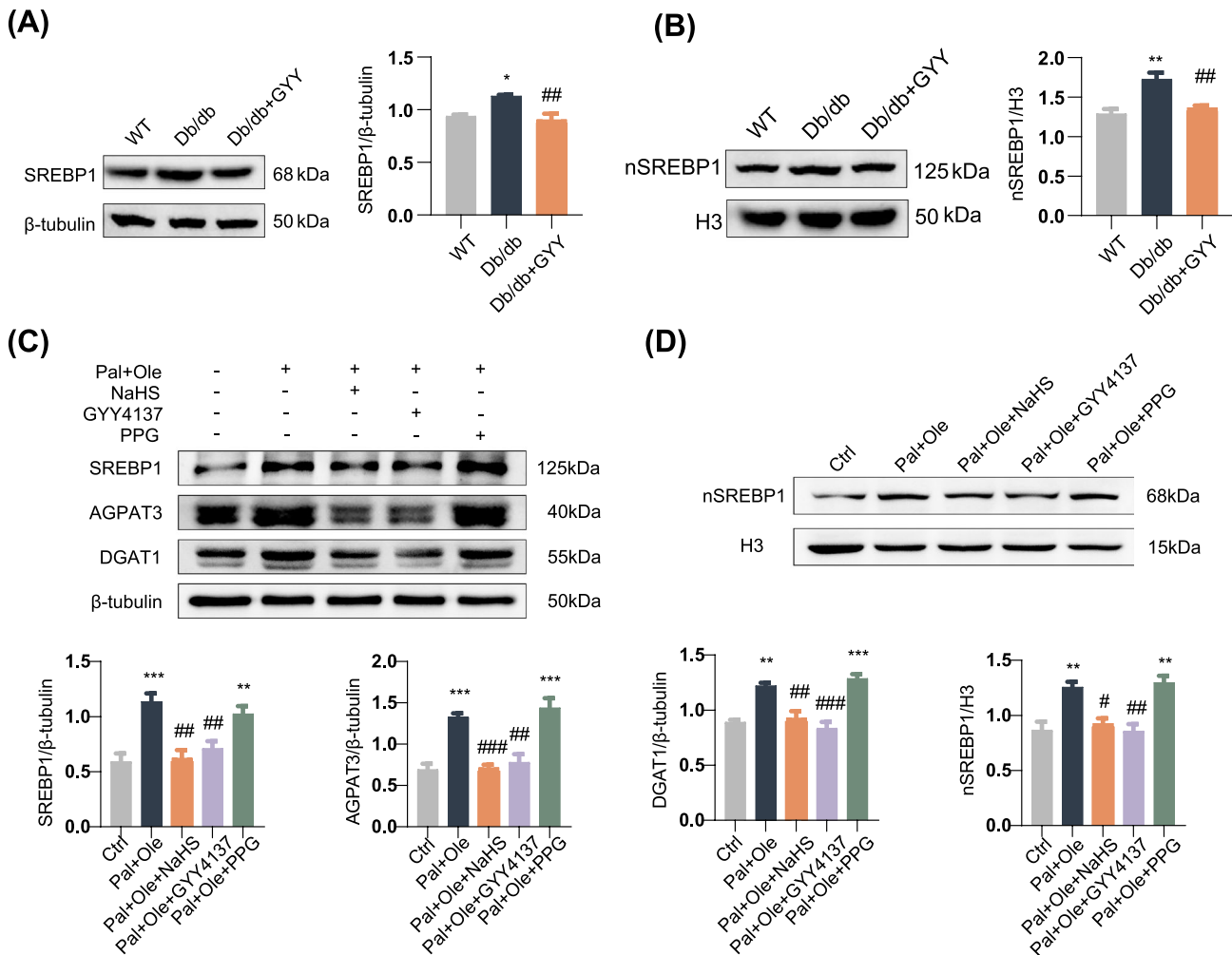
Figure 4 Exogenous H_2S reduced the expression of lipid-related proteins and nSREBP1 translocation to the nucleus. (A, B) Expression of SREBP1 and nuclear SREBP1 (nSREBP1) in db/db mice after treatment with GYY4137 (*n* = 4). (C) Expression of SREBP1, DGAT1 and AGPAT3 in cardiomyocytes (*n* = 4). (D) Expression of nSREBP1 in the nucleus (*n* = 4). Values are presented as mean ± SEM. **$P < 0.01$, ***$P < 0.001$ versus control group, #$P < 0.05$, ##$P < 0.01$, ###$P < 0.001$ versus db/db group or Pal+Ole group.

larly, in the nucleus, we observed an increase in the expression of spliced nSREBP1 in the Pal+Ole group and the Tg group (Figure 6A), while exogenous H_2S and 4-PBA decreased the expression of nSREBP1. These results indicate that exogenous H_2S inhibits SREBP1 expression by alleviating ER stress in cardiomyocytes, thereby reducing the nuclear translocation of SREBP1.

The ubiquitin-proteasome system plays a predominant role in the degradation of SREBP1.[28] To explore the reasons for the changes in SREBP1 expression, we then examined the level of ubiquitination in cardiomyocytes and found that the ubiquitination level was increased in the Pal+Ole group compared with the control and NaHS groups (Figure S7a). This finding led us to further examine the ubiquitination level of SREBP1 using a Co-IP assay. We observed that the ubiquitination level of SREBP1 was clearly reduced in the Pal+Ole group and the Tg group compared with the control group. As ex-

pected, the ubiquitination level of SREBP1 was significantly increased after administration of exogenous H_2S and 4-PBA (Figure 6C). Lysine ubiquitylome analysis showed that 359 proteins were accurately quantified in the hearts of db/db mice compared with the hearts of NaHS-treated db/db mice. Among them, 85 proteins were quantified as down-regulated targets, and 37 proteins were quantified as up-regulated targets when setting a quantification ratio of >1.5 as up-regulated threshold and <0.67 as the down-regulated threshold (Figure 6D). KEGG pathway analysis found that these proteins were involved in cardiac contraction, dilated cardiomyopathy and biosynthesis of amino acids (Figure 6E). Taken together, these results demonstrate that ER stress may trigger increased translocation of SREBP1 into the nucleus via the ubiquitin-proteasome system. However, exogenous H_2S reduced the level of ER stress, thereby decreasing the translocation of SREBP1.
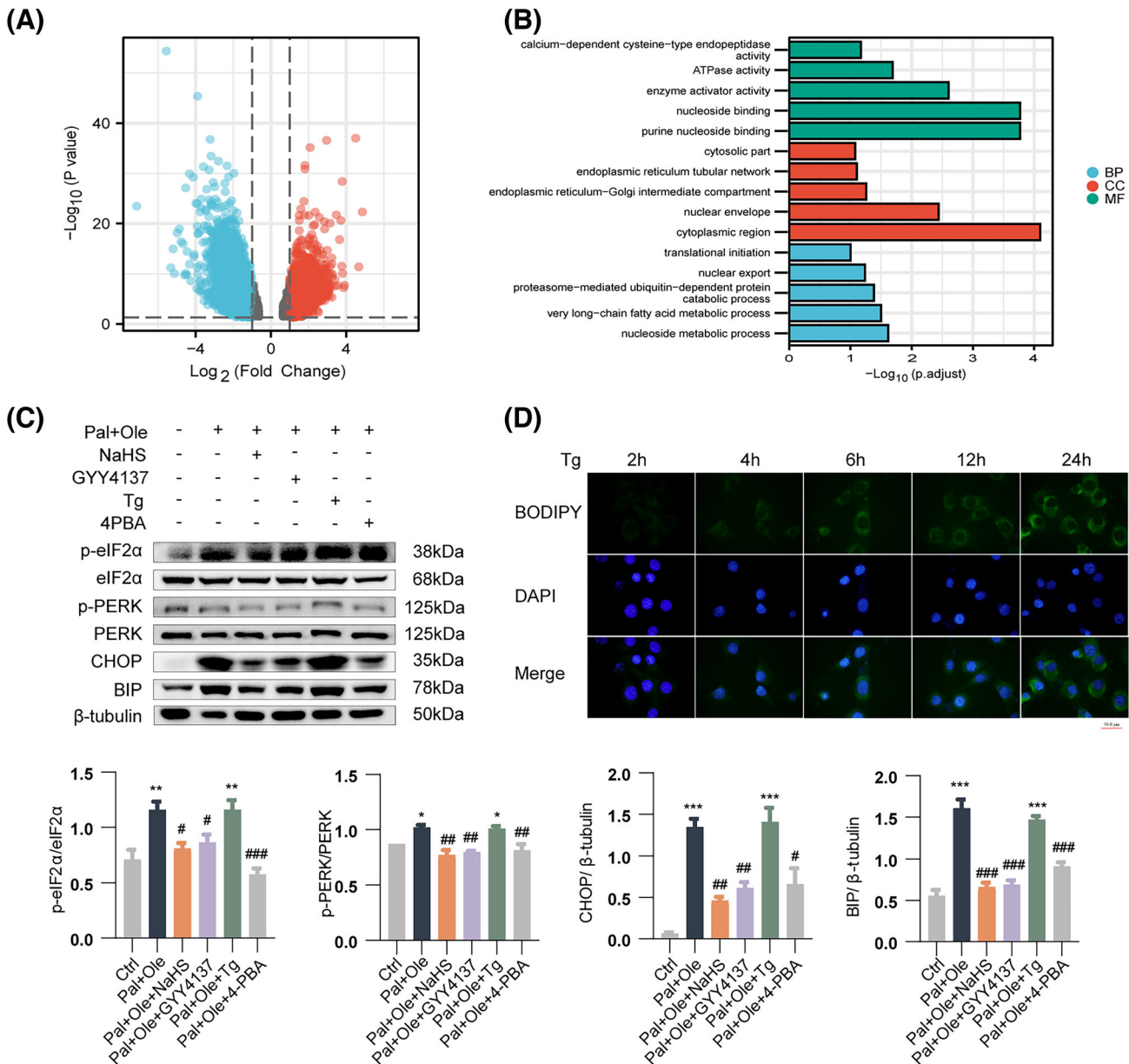
Figure 5 Exogenous H$_2$S decreased the number of LDs by alleviating endoplasmic reticulum stress. (A) Differentially expressed genes are indicated on the volcano plot as a result of the db/db group compared with the control group. (B) Genes were annotated in three main categories: Biological process (BP), cellular component (CC) and molecular function (MF). (C) The expression of ER stress-related proteins in cardiomyocytes (n = 3). (D) The number of LDs in cardiomyocytes at different time points treated with agonists and inhibitors. Values are presented as mean ± SEM. *P < 0.05, **P < 0.01, ***P < 0.001 versus control group, #P < 0.05, ##P < 0.01, ###P < 0.001 versus db/db group or Pal+Ole group.

The E3 ubiquitin ligase SYVN1 is involved in regulating the ubiquitinated degradation of SREBP1

We successfully predicted the E3 ubiquitin ligases of SREBP1 by bioinformatics and found a total of 123 E3 ubiquitin ligases that interact with SREBP1, eight of which had high-confidence interactions.[29] As shown in Figure S8a and

Figure S7b, we have listed the top 10 E3 ubiquitin ligases ranked from high to low confidence scores, of which the highest confidence score is SYVN1.

Immunofluorescence and Co-IP assay showed co-localization between SREBP1 and SYVN1 (Figure 7A, Figure S7c). Molecular docking further corroborated this finding (Figure S8b). Subsequently, we examined SYVN1 expression. The results indicated a reduction in SYVN1 expression
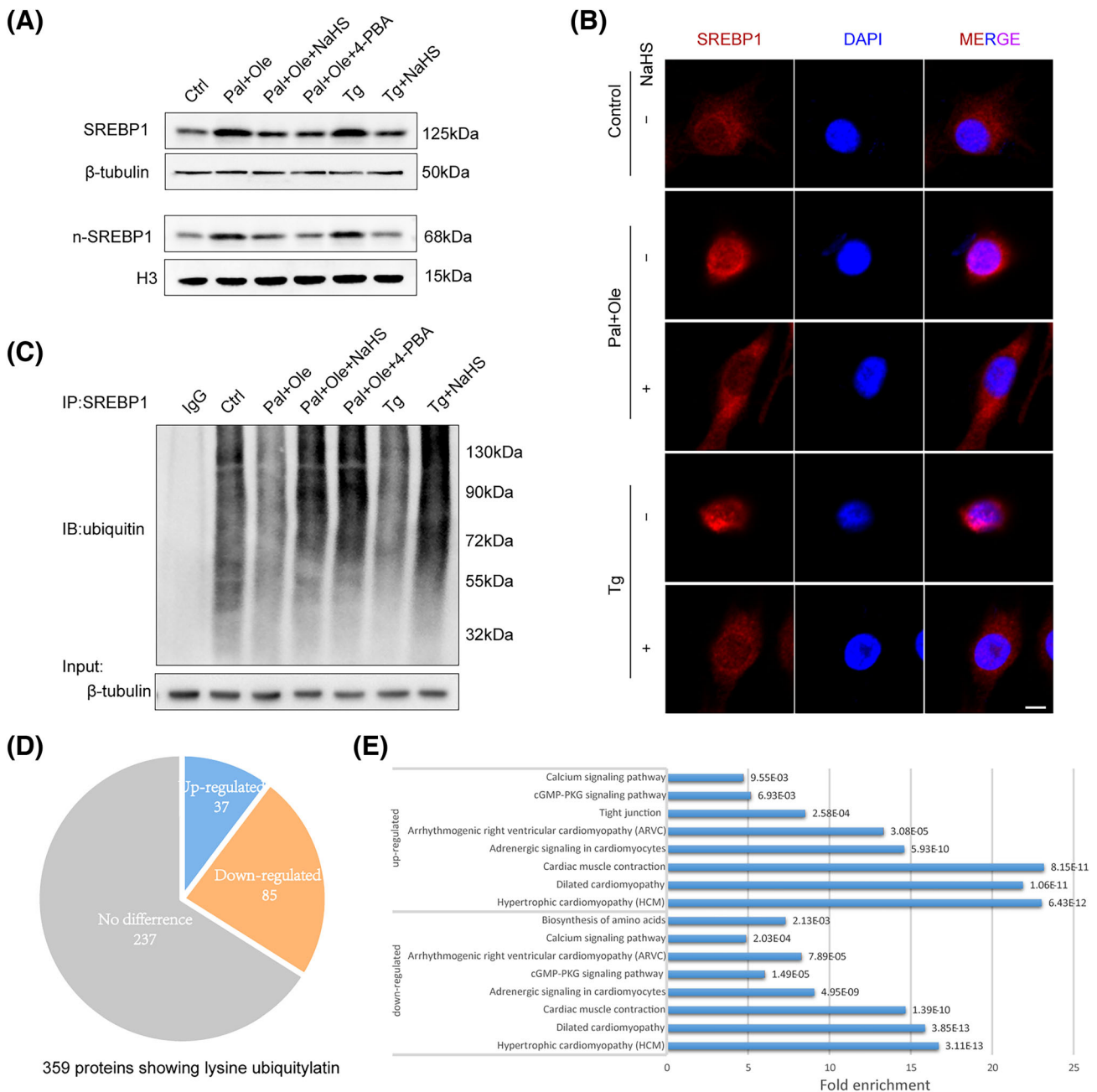
Figure 6 Exogenous H$_2$S reduced SREBP1 expression by attenuating ER stress. (A) The expression of SREBP1 (n = 4) and nSREBP1 (n = 3) was detected by Western blot analysis. (B) Laser confocal microscopy detection of nuclear translocation of SREBP1 (scale bar length: 50 μm). (C) The ubiquitination level of SREBP1 was detected by co-IP and Western blot analysis. (D) Pie chart showing the number of ubiquitylation proteins identified by LC–MS/MS in model db/db mice compared with NaHS-treated db/db mice. (E) KEGG pathway-based enrichment analysis of up- and down-regulated Kub proteins. Values are presented as mean ± SEM. ***P < 0.001 versus control group, #P < 0.05, ##P < 0.01, ###P < 0.001 versus Pal+Ole group.

within the db/db mice. Notably, the administration of GYY4137 and NaHS exhibited significant restorative effects on SYVN1 expression (Figure S8c, d). We further found that compared with the Pal+Ole group, exogenous H$_2$S increased SYVN1 expression in cardiomyocytes and that SYVN1 expression was reduced after administration of Tg (Figure S8e). These results demonstrate that exogenous H$_2$S can promote SYVN1 expression by alleviating the occurrence of ER stress in type 2 diabetic cardiomyocytes and enhancing the ubiquitin-proteasomal degradation of SREBP1.
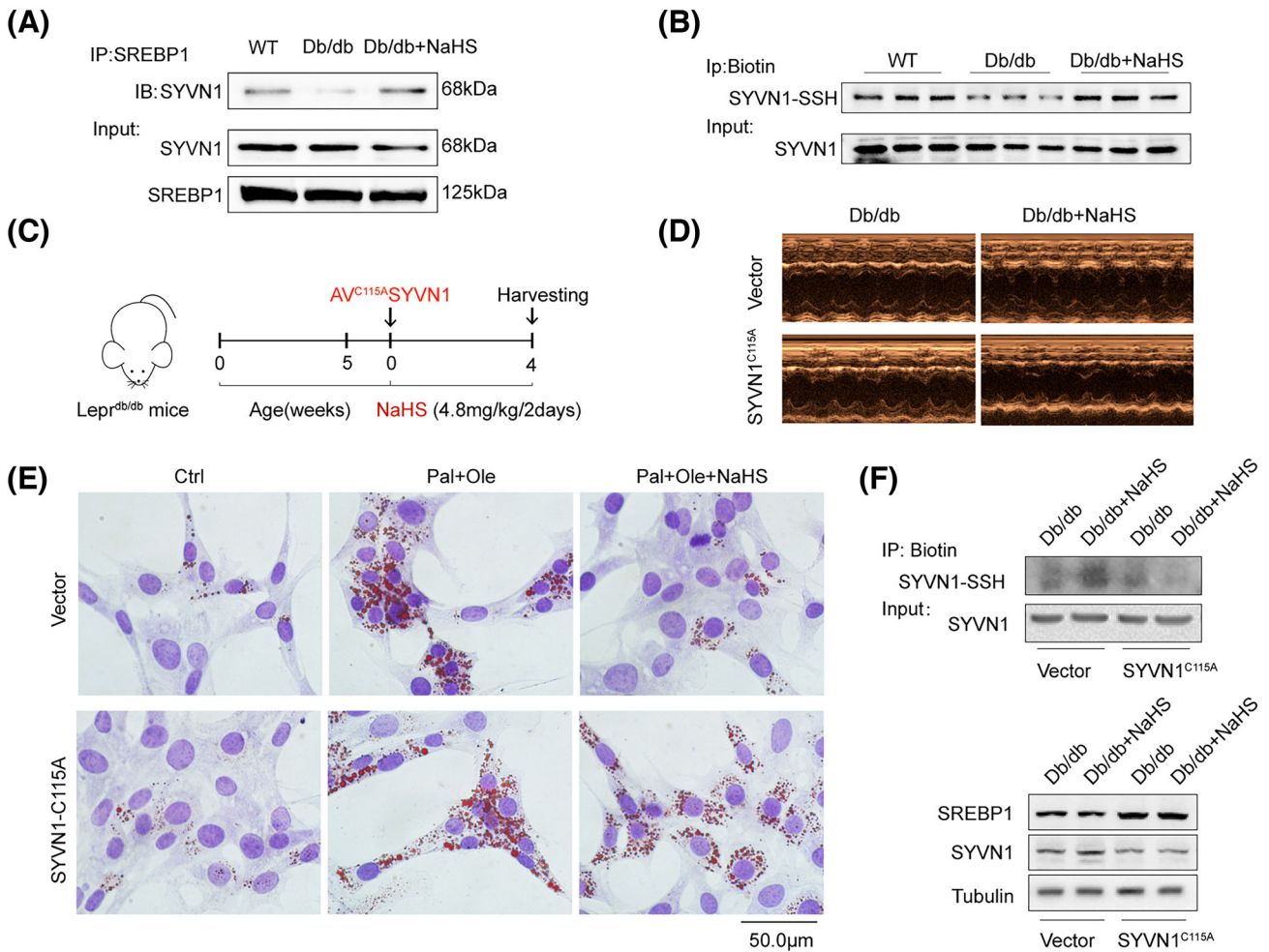
Figure 7 Exogenous H₂S increased SREBP1 ubiquitylation by modifying SYVN1 at Cys115. (A) Immunoprecipitation assay for detecting the interaction between SREBP1 and SYVN1. (B) S-sulfhydration levels of SYVN1 detected by biotin conversion assay. (C) Schematic representation of adenoviral transduction and NaHS treatment in mice. (D) Cardiac ultrasound assessment of mouse cardiac function. (E) LDs were detected by Oil red O staining in HL1 cells. (F) SYVN1 point mutations were transfected to measure SYVN1 sulfhydration levels and the protein expression of SREBP1 and SYVN1.

Exogenous H₂S regulates SREBP1 ubiquitylation by modifying SYVN1 at Cys115

We next investigated how H₂S can decrease the expression of lipid-related proteins. Accumulating evidence has demonstrated that S-sulfhydration, a cysteine-induced posttranslational modification by H₂S, can alter the structure and function of a modified protein and regulate different crucial biological processes.[30] We observed that NaHS can restore the Ssulfhydration level of SYVN1 in db/db mice (Figure 7B, Figure S9a). The cysteine at position 115 is located in the active centre of SYVN1, and Cys115 is relatively conserved in multiple species (Figure S9b, c). To investigate the role of SYVN1 in the degradation of SREBP1, we constructed and transfected SYVN1 mutated at cysteine 115 to alanine (SYVN1-C115A) or wild type into HL-1 cells. As a result, the overexpression of SYVN1C115A did not decrease the expression of SREBP1 and nSREBP1 in HL-1 cells treated with Ole +Pal+NaHS compared with the Pal+Ole group (Figure S9d, e). A Co-IP assay showed that the interaction between SREBP1 and SYVN1 and the ubiquitylation level of SREBP1 in the SYVN1-C115A-overexpressing group administered NaHS were lower than those in the wild-type SYVN1-overexpressing group treated with NaHS (Figure S9f, g). Oil Red O staining also revealed that the number of LDs was not reduced in the SYVN1C115A group treated with NaHS compared with the group without NaHS (Figure 7E).

Transduction of db/db mice with an adenoviral vector carrying the SYVN1-C115A mutant gene revealed that NaHS fails to reverse cardiac function, to restore the expression of SREBP1 and SYVN1, or to alleviate the cysteine S-sulfhydration levels of SYVN1 (Figure 7C,D,F). These

combined findings provide robust support to the notion that exogenous H$_2$S orchestrates an elevation in the ubiquitylation-mediated degradation of SREBP1, a process intricately linked to the modification of SYVN1 at the critical Cys115 site. This concerted molecular modulation ultimately culminates in the curtailment of lipid droplet numbers within cardiomyocytes, a mechanism that holds potential implications for the management of diabetic cardiomyopathy.

Discussion

H$_2$S is a crucial physiological signalling molecule that regulates cardiovascular homeostasis. H$_2$S exerts protective roles in diabetic cardiomyopathy, such as preservation of mitochondrial respiration, maintenance of mitochondrial ATP production and inhibition of cardiomyocyte apoptosis.[31] In this study, we observed significantly decreased levels of H$_2$S and CSE protein expression in cardiac tissues of db/db mice. The number of lipid droplets increased in a time-dependent manner, while exogenous H$_2$S decreased the number of LDs. We showed that the expression of DGAT1 and AGPAT3 and the transcription factor SREBP1, the key enzymes of LD formation, were increased in the cardiac tissues of db/db mice. We reported a novel finding that H$_2$S modulated the interaction between SYVN1 and SREBP1 through SYVN1 S-sulfhydration to elevate SREBP1 ubiquitination to reduce LD formation.

Cellular lipid metabolism and homeostasis are controlled by SREBPs. When SREBPs are aberrantly expressed in cardiomyocytes, they cause ER stress and inflammation.[32] SREBPs originate in the rough ER and associate with ER membrane

protein INSIG1. During heightened cellular metabolism, SREBPs heterodimerize with chaperone protein SCAP, translocating to the Golgi through COPII-coated vesicles. Golgi proteases S1P and S2P process SREBP1, which harbours nuclear localization signals, enabling its entry into the nucleus for transcriptional regulation of lipid-related genes.[33] Using western blot analysis, we found that the expression of SREBP1 and nSREBP1 was significantly increased in cardiac tissues of db/db mice and in cardiomyocytes treated with high palmitate and oleate, while exogenous H$_2$S clearly down-regulated SREBP1 expression.

The unfolded protein response was originally recognized as a conserved adaptive system to protein stress and is currently considered a disturbance to ER homeostasis, commonly referred to as ER stress.[34] SREBPs have been confirmed to be associated with ER stress-mediated lipotoxicity. PERK-mediated eIF2α phosphorylation during ER stress induces INSIG1 degradation, which leads to proteolytic activation of SREBPs.[35] We observed that the ER stress-related proteins BIP, CHOP p-PERK and p-eIF2α were increased, and their expression was clearly decreased after treatment with exogenous H$_2$S. We further investigated SREBP1 expression by modulating ER activity using agonists and inhibitors. Cardiomyocytes treated with Tg exhibited increased SREBP1 expression, which was significantly suppressed by exogenous H$_2$S. To elucidate the mechanism, we assessed cardiomyocyte ubiquitination levels. Pal+Ole treatment globally elevated ubiquitination, yet SREBP1's ubiquitination was reduced in this group. Both exogenous H$_2$S and 4-PBA enhanced SREBP1's ubiquitination, implying ubiquitin-proteasome-mediated degradation. These findings suggest that ER stress-linked pathways regulate SREBP1 degradation.
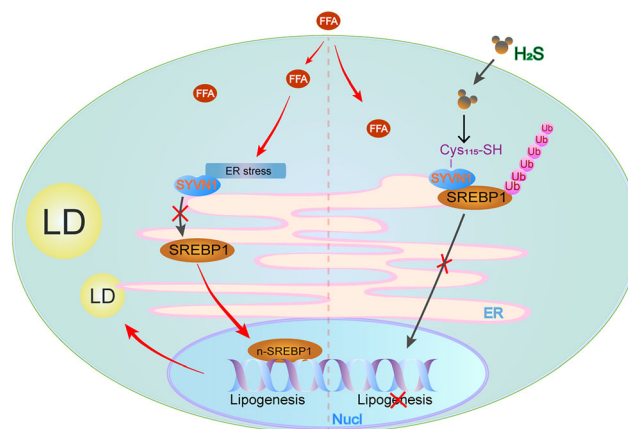

Figure 8 Model for the role of H$_2$S in modifying SYVN1 S-sulfhydration to regulate SREBP1 ubiquitylation and translocation to the nucleus (Nucl). In type 2 diabetic hearts, increased SREBP1 translocation from the endoplasmic reticulum (ER) to the nucleus is involved in ER stress. In addition, H$_2$S mediates S-sulfhydration on SYVN1 (an E3 ubiquitin ligase) at the Cys115 site and increases SREBP1 degradation by the ubiquitination pathway, thereby inhibiting SREBP1 translocation to the nucleus. This inhibition reduces lipogenesis from free fatty acids (FFAs), thus inhibiting the accumulation of lipid droplets (LDs) in diabetic hearts.

Subsequently, we conducted a prediction of the E3 ligase SYVN1 responsible for the degradation of SREBP1. In yeast, the structure of the Dsc complex, which is required for Sre1 (homologues in mammals) and Sre2 cleavage, is similar to that of the SYVN1 E3 ligase complex in mammalian cells.[36] Positive feedback regulation of Sre1 increases the expression of the Sre1 precursor under low oxygen condition, while homeostasis of Sre1 requires the Dsc complex and proteasome to be degraded constantly.[37] Growing evidence has revealed that SYVN1 is important for its physiological functions by recruiting transcription factors for ubiquitination-mediated degradation, including catalysing p53 ubiquitination and PGC-1β ubiquitination.[38] Cysteine S-sulfhydration is a crucial posttranslational modification, where the thiol group (RSH) of the protein cysteine residue is modified to form persulfides (RSSH) and polysulfides (RSS-$_x$H), leading to an increased reactivity of the cysteine residue.[39] These results illustrated that exogenous H2S promoted the ubiquitination-mediated degradation of SREBP1 through SYVN1 S-sulfhydration at cysteine 115 and inhibited SREBP1 nuclear translocation by suppressing the activation of ER stress, thereby reducing the expression of lipid-related genes, ultimately inhibiting lipid accumulation in cardiomyocytes and alleviating lipotoxicity in type 2 diabetic cardiomyopathy.

This study possesses certain limitations. Our current investigation lacks extensive clinical data and cardiac tissue samples. Moreover, further research is needed to explore the regulatory role of exogenous hydrogen sulfide in ER stress.

In conclusion, this study provides compelling evidence that H2S enhances SYVN1 S-sulfhydration and promotes SREBP1 ubiquitination to down-regulate the expression of DGAT1 and AGPAT3 to prevent LDs formation (Figure 8). Our findings suggest that H2S might be a potential therapeutic strategy for diabetic cardiomyopathy.

Data sharing

The data that support the finding of this study are available from the corresponding author upon reasonable request.

Acknowledgements

Funding information

Conflict of interest

The authors declare no conflict of interest.

Data Availability Statement

The data presented in this study are available on request from the corresponding authors.

Online supplementary material

Additional supporting information may be found online in the Supporting Information section at the end of the article.

References

1. Cho NH, Shaw JE, Karuranga S, Huang Y, da Rocha Fernandes JD, Ohlrogge AW, et al. IDF Diabetes Atlas: global estimates of diabetes prevalence for 2017 and projections for 2045. *Diabetes Res Clin Pract* 2018;**138**:271–281.
2. Kannel WB, McGee DL. Diabetes and cardiovascular disease. The Framingham study. *JAMA* 1979;**241**:2035–2038.
3. Ritchie RH, Abel ED. Basic mechanisms of diabetic heart disease. *Circ Res* 2020;**126**:1501–1525.
4. Ruberg FL. Myocardial lipid accumulation in the diabetic heart. *Circulation* 2007;**116**:1110–1112.
5. Nakamura M, Sadoshima J. Cardiomyopathy in obesity, insulin resistance and diabetes. *J Physiol* 2020;**598**:2977–2993.
6. Mallela SK, Ge M, Molina J, Santos JV, Kim JJ, Mitrofanova A, et al. Sphingomyelin phosphodiesterase acid like 3B (SMPDL3b) regulates Perilipin5 (PLIN5) expression and mediates lipid droplet formation. *Genes & Diseases* 2022;**9**:1397–1400.
7. Sharma S, Adrogue JV, Golfman L, Uray I, Lemm J, Youker K, et al. Intramyocardial lipid accumulation in the failing human heart resembles the lipotoxic rat heart. *FASEB J* 2004;**18**:1692–1700.
8. Shimano H, Sato R. SREBP-regulated lipid metabolism: convergent physiology - divergent pathophysiology. *Nat Rev Endocrinol* 2017;**13**:710–730.
9. Eberlé D, Hegarty B, Bossard P, Ferré P, Foufelle F. SREBP transcription factors: master regulators of lipid homeostasis. *Biochimie* 2004;**86**:839–848.
10. Xu D, Wang Z, Xia Y, Shao F, Xia W, Wei Y, et al. The gluconeogenic enzyme PCK1 phosphorylates INSIG1/2 for lipogenesis. *Nature* 2020;**580**:530–535.
11. Shibuya K, Ebihara K, Ebihara C, Sawayama N, Isoda M, Yamamuro D, et al. AAA-ATPase valosin-containing protein (VCP) binds the transcription factor SREBP1 and promotes its proteolytic activation by rhomboid protease RHBDL4. *J Biol Chem* 2022.
12. Wang H, Shi X, Qiu M, Lv S, Zheng H, Niu B, et al. Hydrogen sulfide plays an important role by influencing NLRP3 inflammasome. *Int J Biol Sci* 2020;**16**:2752–2760.
13. Szabo C, Papapetropoulos A. International Union of Basic and Clinical Pharmacology.

CII: pharmacological modulation of H₂S levels: H₂S donors and H₂S biosynthesis inhibitors. *Pharmacol Rev* 2017;**69**: 497–564.

14. Tocmo R, Parkin K. S-1-propenylmercaptocysteine protects murine hepatocytes against oxidative stress via persulfidation of Keap1 and activation of Nrf2. *Free Radic Biol Med* 2019;**143**:164–175.

15. Wu J, Tian Z, Sun Y, Lu C, Liu N, Gao Z, et al. Exogenous H₂S facilitating ubiquitin aggregates clearance via autophagy attenuates type 2 diabetes-induced cardiomyopathy. *Cell Death Dis* 2017;**8**:e2992.

16. da Zhang DJ, Tang C, Huang Y, Jin H. H₂S-induced sulfhydration: biological function and detection methodology. *Front Pharmacol* 2017;**8**:608.

17. Mard SA, Ahmadi I, Ahangarpour A, Gharib-Naseri MK, Badavi M. Delayed gastric emptying in diabetic rats caused by decreased expression of cystathionine gamma lyase and H2 S synthesis: in vitro and in vivo studies. *Neurogastroenterology and Motility: The Official Journal of the European Gastrointestinal Motility Society* 2016;**28**:1677–1689.

18. Bibli S-I, Fleming I. Oxidative post-translational modifications: a focus on cysteine S-sulfhydration and the regulation of endothelial fitness. *Antioxid Redox Signal*.

19. Luo S, Kong C, Zhao S, Tang X, Wang Y, Zhou X, et al. Endothelial HDAC1-ZEB2-NuRD complex drives aortic aneurysm and dissection through regulation of protein S-sulfhydration. *Circulation* 2023;**147**: 1382–1403.

20. Zhou Z, Torres M, Sha H, Halbrook CJ, Bergh FVD, Reinert RB, et al. Endoplasmic reticulum-associated degradation regulates mitochondrial dynamics in brown adipocytes. *Science (New York, NY)* 2020;**368**: 54–60.

21. Sun Y, Zhang L, Lu B, Wen J, Wang M, Zhang S, et al. Hydrogen sulphide reduced the accumulation of lipid droplets in cardiac tissues of db/db mice via Hrd1 S-sulfhydration. *J Cell Mol Med* 2021;**25**: 9154–9167.

22. Meng G, Zhao S, Xie L, Han Y, Ji Y. Protein S-sulfhydration by hydrogen sulfide in cardiovascular system. *Br J Pharmacol* 2018; **175**:1146–1156.

23. Fiorucci S, Distrutti E, Cirino G, Wallace JL. The emerging roles of hydrogen sulfide in the gastrointestinal tract and liver. *Gastroenterology* 2006;**131**:259–271.

24. Han J, Li E, Chen L, Zhang Y, Wei F, Liu J, et al. The CREB coactivator CRTC2 controls hepatic lipid metabolism by regulating SREBP1. *Nature* 2015;**524**:243–246.

25. Jia G, DeMarco VG, Sowers JR. Insulin resistance and hyperinsulinaemia in diabetic cardiomyopathy. *Nat Rev Endocrinol* 2016; **12**:144–153.

26. Ozcan U, Cao Q, Yilmaz E, Lee A-H, Lwakoshi NN, Ozdelen E, et al. Endoplasmic reticulum stress links obesity, insulin action, and type 2 diabetes. *Science (New York, NY)* 2004;**306**:457–461.

27. Yuan X, Cai C, Chen S, Yu Z, Balk SP. Androgen receptor functions in castration-resistant prostate cancer and mechanisms of resistance to new agents targeting the androgen axis. *Oncogene* 2014;**33**: 2815–2825.

28. Punga T, Bengoechea-Alonso MT, Ericsson J. Phosphorylation and ubiquitination of the transcription factor sterol regulatory element-binding protein-1 in response to DNA binding. *J Biol Chem* 2006;**281**: 25278–25286.

29. Li Y, Xie P, Lu L, Wang J, Diao L, Liu Z, et al. An integrated bioinformatics platform for investigating the human E3 ubiquitin ligase-substrate interaction network. *Nat Commun* 2017;**8**:347.

30. Bibli S-I, Hu J, Looso M, Weigert A, Ratiu C, Wittig J, et al. Mapping the endothelial cell S-sulfhydrome highlights the crucial role of integrin sulfhydration in vascular function. *Circulation* 2021;**143**:935–948.

31. Li Z, Xia H, Sharp TE, LaPenna KB, Elrod JW, Casin KM, et al. Mitochondrial H₂S regulates BCAA catabolism in heart failure. *Circ Res* 2022;**131**:222–235.

32. Kim JY, Wang LQ, Sladky VC, Oh TG, Liu J, Trinh K, et al. PIDDosome-SCAP crosstalk controls high-fructose-diet-dependent transition from simple steatosis to steatohepatitis. *Cell Metab* 2022;**34**: 1548–1560.e6.

33. Ferré P, Phan F, Foufelle F. SREBP-1c and lipogenesis in the liver: an update1. *Biochem J* 2021;**478**:3723–3739.

34. Oakes SA, Papa FR. The role of endoplasmic reticulum stress in human pathology. *Annu Rev Pathol* 2015;**10**:173–194.

35. Kim JY, Garcia-Carbonell R, Yamachika S, Zhao P, Dhar D, Loomba R, et al. ER stress drives lipogenesis and steatohepatitis via caspase-2 activation of S1P. *Cell* 2018;**175**: 133–145.e15.

36. Stewart EV, Nwosu CC, Tong Z, Roguev A, Cummins TD, Kim DU, et al. Yeast SREBP cleavage activation requires the Golgi Dsc E3 ligase complex. *Mol Cell* 2011;**42**: 160–171.

37. Hughes BT, Nwosu CC, Espenshade PJ. Degradation of sterol regulatory element-binding protein precursor requires the endoplasmic reticulum-associated degradation components Ubc7 and Hrd1 in fission yeast. *J Biol Chem* 2009;**284**:20512–20521.

38. Xu Y, Fang D. Endoplasmic reticulum-associated degradation and beyond: the multitasking roles for HRD1 in immune regulation and autoimmunity. *J Autoimmun* 2020;**109**:102423.

39. Gupta R, Sahu M, Tripathi R, Ambasta RK, Kumar P. Protein S-sulfhydration: unraveling the prospective of hydrogen sulfide in the brain, vasculature and neurological manifestations. *Ageing Res Rev* 2022;**76**:101579.